NUMERICAL MODELING OF THE AUSTRALASIAN TEKTITE STREWN FIELD. N. Artemieva[1,2], [1]Planetary Science Institute, 1700 E.Ft.Lowell, Tucson, AZ, artemeva@psi.edu, [2]Institute for Dynamics of Geospheres, Moscow, Russia

Introduction The biggest and the youngest tektite strewn field, Australasian [1,2], is the single strewn field on Earth for which the parent crater is still not identified, although many researches point to a relatively small area in Indochina (104-109°E, 10-17°N, Table ## in [3]. This strewn field contains all known types of tektites (splash-form, ablated, Myong Nong) as well as microtektites. Recent findings of microtektites in Antarctica [4] increase the strewn field size substantially. An estimated total mass of Australasian tektites (AAT) ranges from 10^{11} kg [5] to $2 \cdot 10^{12}$ kg [6], and up to $3.2 \cdot 10^{13}$ kg [7]; parent crater size varies from the first tens of km up to 300 km.

Due to the fact that such a big parent crater remains unknown, it is reasonable to suggest that it was destroyed by water currents immediately after its formation on the oceanic shelf. This assumption is consistent with publications [9, 11-12]. On one hand, ^{10}Be content in tektites [3] and the results of numerical modeling [13] demand a very shallow initial depth of tektite-forming sediments. On the other hand, the presence of a water layer (and/or water-saturated sediments) leads to a higher ejection velocities, and, finally, to a wider distribution of ejecta. In particular, the recent drilling project and numerical modeling of the Chesapeake Bay structure [14] confirmed that North-American tektites have been ejected from a crater covered by water. The main goals of this paper are: (1) to estimate the minimal crater size, allowing production of reasonable amount of AAT; (2) to discuss post-impact evolution of this crater and possible geophysical signatures which can help to identify its remnants.

Numerical model and initial conditions. We model high-velocity phenomena with the 3D hydrocode SOVA [15] complemented by the ANEOS equation of state for geological materials [16-17]. In three separate stages we reproduce: 1) the impact and initial ejection of material; 2) the ballistic continuation of ejecta on a sphere; and 3) ejecta as it re-enters the atmosphere. Tracer particles are used to find the maximum shock compression and an initial depth of target materials. Ejecta may be considered as potential tektites if shock compression is above 30-40 GPa [18].

Impact velocity is equal to 18 km/s, impact angles are 30° and 45° to horizon. The minimal water depth should exceed the crater rim height [19] to allow immediate and strong resurge. The maximum water depth should not exceed the depth of melting of the oceanic floor (2-3 times the projectile diameter [20]). Fig. 1 shows these estimates for a wide range of projectile sizes as well as the initial conditions of computational models (black symbols: S – 300-m-dameter projectile; M – 1-km-diameter; L – 5-km-diameter asteroid). To compare the results with a crater-forming impact on acontinent, we model an impact of a 1-km-diameter asteroid without a water layer (MD).

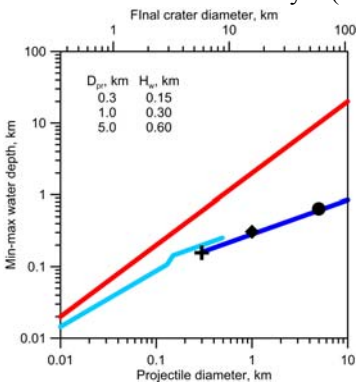

Fig.1. Estimates of (1) minimal water depth allowing a water surge into the final crater – light blue and dark blue curves (iron and stony projectiles, respectively); (2) maximum water depth allowing melting of sediments at the bottom. Also shown are initial conditions for the model (black symbols and the text).

Results. The initial (immediately following the ejection) distribution of molten ejecta over velocities is shown in Fig. 2. Obviously, the presence of a 300-m-thick water layer leads to a substantial decrease in the amount of high-velocity (>5 km/s) ejecta, and to total absence of ejecta with velocities above 7 km/s. However, the total mass of ejecta with velocities >1 km/s is ~ $4 \cdot 10^{12}$ kg, which complies with geological estimates [6]. After a larger impact, this mass is 100 times bigger (and an order of magnitude bigger than the maximum geological guess [7]).

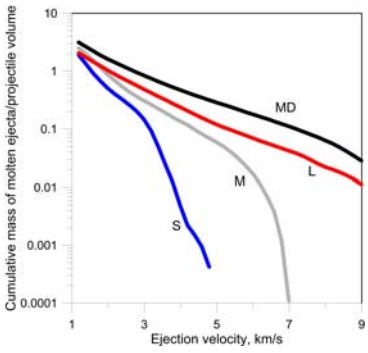

Fig. 2. Cumulative distribution of ejected mass divided by projectile mass for all variants.

If we exclude sediments which were initially deeper than 200 m, then the total mass decreases tenfold. After the smallest impact under consideration the mass of ejecta with velocities > 3km/s is ten times smaller than the projectile mass, i.e., < $3.5 \cdot 10^9$ кg. Obviously, this small impact (and, hence, an impact crater smaller than 10 km) may be excluded from this study.

Final distributions of microtektites for various scenarios are compared in Figs. 3 and 4. To produce these maps we assumed that (1) microtektites prevail by mass (what may be not the case at proximal sites

where larger tektites are frequent); (2) average diameter of microtektites is 267 μm [8]. At large distances (>1000 km) distributions are strongly asymmetric with the majority of molten materials in a downrange direction and with a prominent ray system; proximal deposits are symmetric. A decrease of the impact angle (Fig. 3) leads to a slightly longer and narrower strewn field, although these differences may be difficult to identify in the field. An impact into continental crust produces a larger strewn field (Fig. 4) albeit with similar concentration of tektites at distances <10,000 km. All these scenarios are qualitatively consistent with observations. Distribution of tektites after a large impact is similar to MD-45 in size and shape with 100 times higher concentration of micotektites.

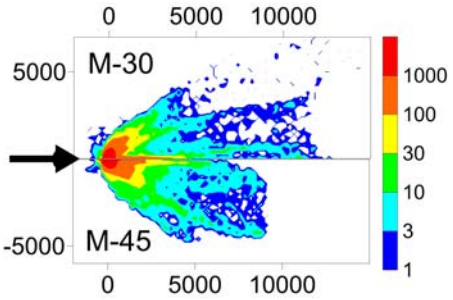

Fig. 3. Number of microtektites per 1 cm^2 as a function of a distance (in km) from the impact point (0,0). Only half of the "map" for each variant is depicted. A black arrow shows the impact direction. M-30: a 1-km-diameter asteroid striking at a 30° to horizon into a 300-m-deep water layer; M-45: same projectile size, but the impact angle is 45°.

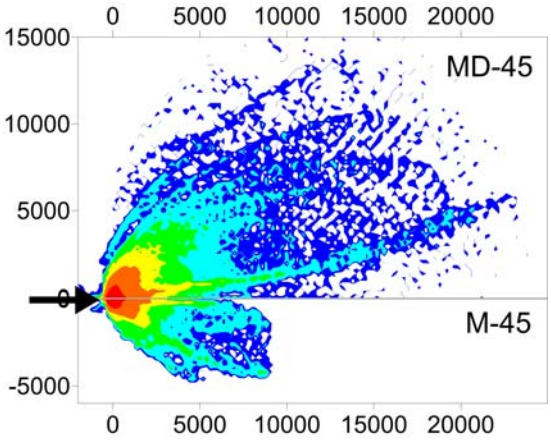

Fig. 4. Comparison of a 45 impact into a 300-m-deep water layer (M-45) and into a dry surface (MD-45). All colors are the same as in Fig.3.

Berillium-10 in tektites. Fig. 5 shows the average initial depth of ejected melt as a function of its final distance from the parent crater. This depth may be directly connected to a ^{10}Be concentration in tektites although the exact concentration of this isotope in soils strongly depends on sedimentation rate and other conditions [3]. Our results show a strong decrease of this depth (and hence, an increase in ^{10}Be content) with distance. Average shock compression of melts increases with the increasing distance, i.e., average tektites' size should decrease with no tektites (but microtektites) beyond 8,000 km.

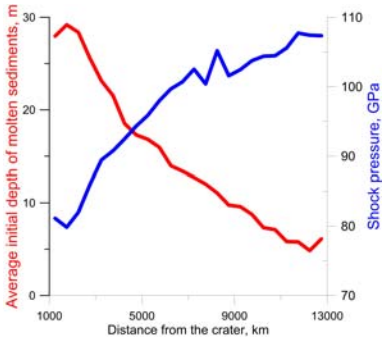

Fig. 5. Initial depth of molten material (red line and left axis) its and maximum shock compression (blue line and right axis) as a function of distance from the parent crater.

Conclusions: Numerical models show that the AAT strewn field may be produced by a ~1-km-diameter asteroid into the oceanic shelf with the final crater diameter of ~20 km. Geophysical signatures may be similar to the Mjolnir marine impact crater [21].

References: [1] Koeberl C. (2007) *Treatise of Geochemistry*,.1.28.1-1.28.52. [2] Glass B. P. and Koeberl C. (2006) *Meteoritics and Plan. Sci. 41*, 305-326. [3] Ma P. et al. (2004) *Geochim. Cosmochim. Acta 68*, 3883-3896. [4] Folco L. et al. (2008) *Geology 36*, 291-294. [5] Glass B.P. (1990) *Tectonophysics 171*, 393-404. [6] Koeberl C. (1994) *Geol. Soc. America Special Paper 293*, 133–151. [7] Schmidt G. et al. (1993) *Geochim. Cosmochim. Acta 57*, 4851–4859. [8] Glass B.P. and Pizzuto J.E. (1994) *JGR 99*, 19,075-19,081. [9] Schnetzler C.C. et al. (1988) *GRL 15*, 15,357-360. [10] Hartung J. and Koeberl C. (1994) *Meteoritics 29*, 411–416. [11] Chaussidon M. and Koeberl C. (1995) *Geochim. Cosmochim. Acta 59*, 613–624. [12] Stecher O. et al. (2009). *AGU Fall Meeting*, Abstract #NH33A-1134. [13] Stöffler D. et al. (2002). *Meteoritics and Plan. Sci. 37*, 1893-1907. [14] Kenkmann Th. et al. (2009). *Geol. Soc. America Special Paper 458*, 571-585. [15] Shuvalov V.V. (1999) *Shock Waves 9*, 381–390. [16] Thompson S. L. and Lauson H .S. (1972) *Report SC-RR-71 0714.* 119 p. [17] Melosh H. J. (2007) *Meteoritics & Plan. Sci. 42*, 2079-2098. [18] Wünnemann K. et al. (2008) *EPSL 269*, 530-539. [19] Collins G.S. et al. (2005) *Meteoritics & Plan. Sci. 40*, 817-840. [20] Artemieva N.A. and Shuvalov V.V. (2002) *Deep Sea Research Part II: Topical Studies in Oceanography 40*, 959-968. [21] Shuvalov V. et al. (2002). *JGR 107*, doi: 10.1029/2001JE001698